

Myriad: a real-world testbed to bridge trajectory optimization and deep learning

Nikolaus H. R. Howe
Mila, Université de Montréal
niki.howe@mila.quebec

Simon Dufort-Labbé
Mila, Université de Montréal

Nitarshan Rajkumar
University of Cambridge*

Pierre-Luc Bacon
Mila, Université de Montréal, Facebook CIFAR AI, IVADO.

Abstract

We present Myriad, a testbed written in JAX for learning and planning in real-world continuous environments. The primary contributions of Myriad are threefold. First, Myriad provides machine learning practitioners access to trajectory optimization techniques for application within a typical automatic differentiation workflow. Second, Myriad presents many real-world optimal control problems, ranging from biology to medicine to engineering, for use by the machine learning community. Formulated in continuous space and time, these environments retain some of the complexity of real-world systems often abstracted away by standard benchmarks. As such, Myriad strives to serve as a stepping stone towards application of modern machine learning techniques for impactful real-world tasks. Finally, we use the Myriad repository to showcase a novel approach for learning and control tasks. Trained in a fully end-to-end fashion, our model leverages an implicit planning module over neural ordinary differential equations, enabling simultaneous learning and planning with complex environment dynamics.

1 Introduction

The rapid progress of machine learning (ML) algorithms is made clear by the yearly improvement we see on standard ML testbeds (Deng et al., 2009; Todorov et al., 2012; Bellemare et al., 2013). Inevitably, the popularity of a given benchmark creates a positive feedback effect, encouraging researchers to develop algorithms that achieve good performance on that set of tasks (Kerner, 2020; Henderson et al., 2018). We believe it is crucial that our algorithms be well-suited for positive-impact, real-world applications. As such, we must be able to train and test them on real-world-relevant tasks.

To this end, we present Myriad¹, a real-world testbed for optimal control methods, such as imitation learning and reinforcement learning (RL). Myriad differs from previous testbeds in several key aspects. First, and most importantly, all tasks are inspired by real-world problems, with applications in health, computational sustainability and epidemiology. Second, Myriad is, to our knowledge, the first repository that enables deep learning methods to be combined seamlessly, and in an end-to-end fashion, with more traditional trajectory optimization methods.

While the field of control theory has yielded practical approaches to solve a plethora of problems in the industrial setting, adoption of such methods within the ML community has been limited. This is in part due to the historical focus of ML on scalability, and of control theory on robustness and optimality, and is further exacerbated by the lack of tools to run control algorithms in a deep learning setting. Yet, trajectory optimization techniques can bring a new perspective into machine learning tasks. For example, many trajectory optimization algorithms allow for constraints to be imposed on the state and control trajectories. This ability to impose safety constraints is crucial in real-world applications, but is difficult to achieve within the standard RL framework: either due to

*Work done while at Mila, Université de Montréal.

¹<https://github.com/nikihowe/myriad>

reward hacking (Betts, 2010; Biegler, 2010; Leike et al., 2018) or limited expressivity of an alternate formulation such as that of Altman (1999).

Additionally, the Myriad repository allows for the combination of trajectory optimization and deep learning techniques into powerful hybrid algorithms. As an example, we implement an imitation learning agent that leverages a control-oriented inductive bias to learn optimal trajectories. This inductive bias is generated by solving an implicit planning problem using trajectory optimization, and is fully differentiable.

Finally, the system dynamics in Myriad are continuous in time and space, offering several advantages over discretized environments. On the one hand, these algorithms are adaptable to varying and even irregularly-spaced data frequencies. This circumvents the possibility to bias an algorithm to a given frequency, and avoids the need to interpolate or discard observations (Chen et al., 2018). It also empowers the agent to increase or decrease sampling frequency as the task demands. At the same time, using continuous-time dynamics means we get to choose between integration techniques. Not only does this give more freedom to the user; it also opens the door to efficient variable-step integration methods, which can take advantage of the local environment dynamics to effectively trade off speed and accuracy of integration (Fehlberg, 1969).

We believe that this combination of features makes Myriad a useful addition to the ML testbed landscape. While there already exist ML testbeds for real-world tasks (Koh et al., 2021), Myriad is to our knowledge the first to focus on learning and control, and to leverage trajectory optimization in a deep learning context. There also exists a rich collection of trajectory optimization testbeds, primarily for robotics, which one might want to build on, instead of developing a new testbed (Antony, 2018; Tedrake et al., 2019). Yet, these testbeds are typically non-differentiable and rely on external solvers for optimization, making them challenging or impossible to integrate in a deep learning workflow and onto deep learning hardware. Myriad bridges the fields of deep learning and optimal control with a collection of fully differentiable algorithms and real-world tasks, all running in a modern ML framework (Bradbury et al., 2018).

This rest of this manuscript is structured as follows. **Section 2** presents an overview of the Myriad testbed. **Section 3** describes two techniques central to trajectory optimization. **Section 4** shows how we can use GPU-accelerated first-order techniques to solve the nonlinear programs derived from trajectory optimization, and how we can include inequality constraints during optimization. **Section 5** presents the system identification problem, and how the Myriad repository can be used to learn neural ordinary differential equation models (Chen et al., 2018) describing arbitrary system dynamics. **Section 6** presents a new deep imitation learning algorithm which includes a control-oriented inductive bias, trained end-to-end using tools from the Myriad repository.

2 Myriad: Environments and Optimizers

The Myriad repository implements dynamical systems spanning biology, medicine, and engineering. These are presented in Table 1 in Appendix A. Myriad is implemented in JAX (Bradbury et al., 2018) and developed with the machine learning community in mind. The repository contains implementations of various trajectory optimization techniques, including single and multiple shooting (Betts, 2010), trapezoidal and Hermite-Simpson collocation (Kelly, 2017), and the indirect forward-backward sweep method (Lenhart and Workman, 2007). Along with trajectory optimization, we also offer algorithms for learning the dynamics of the environment: to learn (identify) the unknown parameters of an a priori model, or those of a black-box neural ordinary differential equation (Neural ODE) model (Chen et al., 2018).

With the exception of off-the shelf nonlinear program solvers such as `ipopt` (Wächter and Biegler, 2006) and `SLSQP` (Virtanen et al., 2020) (Wächter and Biegler, 2006; Virtanen et al., 2020), every aspect of the systems and trajectory optimizers is differentiable, allowing flexible learning and optimization, and easy incorporation in a deep learning practitioner’s workflow.

The repository is extensible, enabling straightforward addition of new environments, trajectory optimization techniques, nonlinear program solvers, and integration methods to the repository:

- We consider *control environments* (which we also call “systems”) specified by their dynamics function, cost function, start state, and final time. A system can optionally include an end state, a terminal cost function, and bounds on the state and controls. In order to create a

new system, the user can extend `FiniteHorizonControlSystem`, an abstract class defined in `systems/base.py`. A list of the environments currently available in Myriad is shown in Appendix A.

- A *trajectory optimizer* has an objective function, a constraint function, control and state bounds, an initial decision variable guess, and an unravel function for sorting the decision variable array into states and controls. To implement a trajectory optimizer, the user can extend the abstract class `TrajectoryOptimizer`, an abstract class defined in `optimizers/base.py`. A list of the trajectory optimizers currently available in Myriad is also given in Appendix A.
- A *nonlinear program solver* is set to have the same function signature as those used by standard off-the-shelf solvers such as `ipopt` and `SLSQP`. To implement a new trajectory optimizer, the user can create a function with the same signature as those in `nlp_solvers`.

3 Trajectory Optimization Methods

Many control problems can be formulated in the language of trajectory optimization, in which we want to find a control trajectory which minimizes an integrated cost. Optionally, we can also require the control signal to drive the system to a desired final state while satisfying constraints on the control and state trajectory. Here we will consider two standard techniques, which play a central role in Myriad: direct single shooting (Betts, 2010), and direct multiple shooting (Betts, 2010). Such *direct* methods have in common that they both *transcribe* the original continuous-time control problem into an approximate nonlinear program analogue.

Letting \mathbf{u} and \mathbf{x} represent control and state functions, c the instantaneous cost and f the system dynamics, the trajectory optimization problem can be written as

$$\begin{aligned}
& \min_{\mathbf{u}(t) \forall t \in [t_s, t_f]} \int_{t_s}^{t_f} c(\mathbf{x}(t), \mathbf{u}(t), t) dt \\
& \text{such that } \dot{\mathbf{x}}(t) = f(\mathbf{x}(t), \mathbf{u}(t)) \forall t \in [t_s, t_f] \\
& \text{with } \mathbf{x}(t_s) = \mathbf{x}_s \\
& \text{and}^* \mathbf{x}(t_f) = \mathbf{x}_f \\
& \text{and}^* \mathbf{x}_{\text{lower}}(t) \leq \mathbf{x}(t) \leq \mathbf{x}_{\text{upper}}(t) \forall t \in [t_s, t_f] \\
& \text{and}^* \mathbf{u}_{\text{lower}}(t) \leq \mathbf{u}(t) \leq \mathbf{u}_{\text{upper}}(t) \forall t \in [t_s, t_f]
\end{aligned} \tag{1}$$

where asterisks indicate optional constraints. Note that we allow time-dependent cost, but assume time-independent dynamics. The simplest and often best approach to find suitable controls is direct single shooting (Betts, 2010). First, we augment the system dynamics with the instantaneous cost:

$$f_{\text{aug}}(\mathbf{x}(t), \mathbf{u}(t), t) = \begin{bmatrix} f(\mathbf{x}(t), \mathbf{u}(t)) \\ c(\mathbf{x}(t), \mathbf{u}(t), t) \end{bmatrix}. \tag{2}$$

Then the integral

$$\begin{bmatrix} \mathbf{x}_s \\ 0 \end{bmatrix} + \int_{t_s}^{t_f} f_{\text{aug}}(\mathbf{x}(t), \mathbf{u}(t), t) dt = \begin{bmatrix} \mathbf{x}_f \\ c_f \end{bmatrix} \tag{3}$$

will contain the integrated cost – the objective we want to minimize – as its final entry. Let ψ be a function which, given a sequence of controls and a timestamp, returns an interpolated control value².

Letting $\mathbf{x}(t_s) = \mathbf{x}_s$ and $c(t_s) = 0$, we can construct the following nonlinear program (NLP):

$$\begin{aligned}
& \text{decision variables } \hat{\mathbf{u}}_0, \hat{\mathbf{u}}_1, \hat{\mathbf{u}}_2, \dots, \hat{\mathbf{u}}_N \\
& \text{objective } \left[\int_{t_s}^{t_f} f_{\text{aug}} \left(\begin{bmatrix} \mathbf{x}(t) \\ c(t) \end{bmatrix}, \psi(\hat{\mathbf{u}}_{0:N}, t), t \right) dt \right] [-1] \\
& \text{equality constraints}^* \mathbf{x}_f = \mathbf{x}_s + \int_{t_s}^{t_f} f(\mathbf{x}(t), \psi(\hat{\mathbf{u}}_{0:N}, t)) dt \\
& \text{inequality constraints}^* \mathbf{u}_i^{\text{lower}} \leq \hat{\mathbf{u}}_i \leq \mathbf{u}_i^{\text{upper}} \quad \text{for } i = 0, \dots, N
\end{aligned} \tag{4}$$

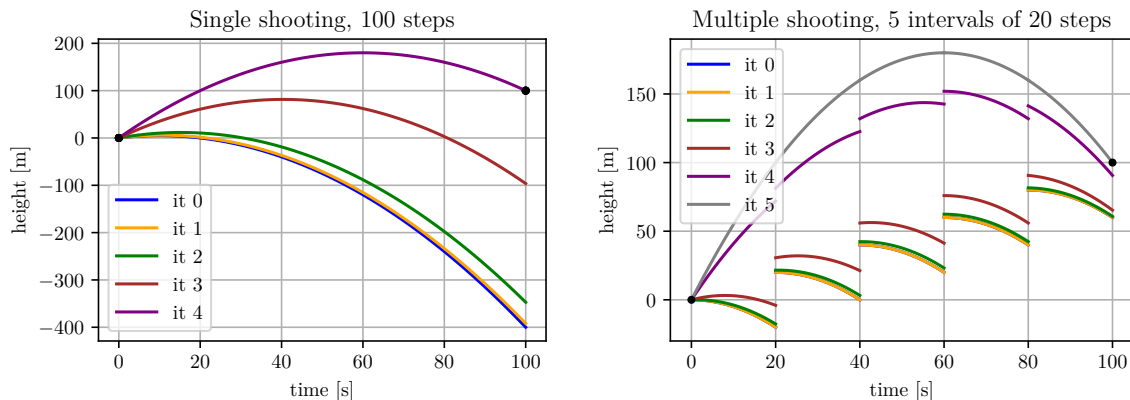
²How this interpolation is performed depends on the integration method applied. Matching the control discretization with a fixed integration timestep circumvents the need for explicit interpolation.

For an application of this method to a pest population dynamics control example (Lenhart and Workman, 2007), see Figure 2. Unfortunately, the direct single shooting approach does not allow us to impose constraints on the state trajectory, and is inherently sequential. Direct multiple shooting addresses both these shortcomings by breaking the problem into a sequence of *shooting intervals* on which direct single shooting can be applied in parallel:

$$\begin{aligned}
& \text{decision variables} && \hat{\mathbf{x}}_0, \hat{\mathbf{x}}_k, \hat{\mathbf{x}}_{2k}, \dots, \hat{\mathbf{x}}_{N-k}, \hat{\mathbf{x}}_N, \hat{\mathbf{u}}_0, \hat{\mathbf{u}}_1, \hat{\mathbf{u}}_2, \dots, \hat{\mathbf{u}}_N \\
& \text{objective} && \left[\sum_{j=1}^{N/k} \int_{t_{(j-1)k}}^{t_{jk}} f_{\text{aug}} \left(\begin{bmatrix} \mathbf{x}(t) \\ c(t) \end{bmatrix}, \psi(\hat{\mathbf{u}}_{(j-1)k:j_k}, t), t \right) dt \right] [-1] \\
& \text{equality constraints} && \hat{\mathbf{x}}_{ik} = \hat{\mathbf{x}}_{(i-1)k} + \int_{t_{(i-1)k}}^{t_{ik}} f(\mathbf{x}(t), \psi(\hat{\mathbf{u}}_{(i-1)k:ik}, t)) dt \quad \text{for } i = 1, 2, \dots, N/k \quad (5) \\
& && \hat{\mathbf{x}}_0 = \mathbf{x}_s \\
& && * \hat{\mathbf{x}}_N = \mathbf{x}_f \\
& \text{inequality constraints}^* && \mathbf{x}_{ik}^{\text{lower}} \leq \hat{\mathbf{x}}_{ik} \leq \mathbf{x}_{ik}^{\text{upper}} \quad \text{for } i = 0, 1, \dots, N/k \\
& && * \mathbf{u}_i^{\text{lower}} \leq \hat{\mathbf{u}}_i \leq \mathbf{u}_i^{\text{upper}} \quad \text{for } i = 0, 1, \dots, N
\end{aligned}$$

State bounds can be enforced at the boundaries of each shooting interval – a significant improvement over single shooting. This can be further refined by decreasing the lengths of the shooting intervals, at the cost of adding more decision variables to the problem.

To gain more intuition about direct single and multiple shooting, we visualize a toy problem of projectile motion, in which we are trying to get a projectile to an altitude of 100m after exactly 100s by choosing a launch velocity. Under simplifying assumptions, given state $\mathbf{x} = [x, \dot{x}]^\top$, the dynamics can be written as $f(\mathbf{x}) = [\dot{x}, -g]^\top$, where g is gravitational acceleration. Figure 1 shows the outcome of applying single and multiple shooting to this problem. Other optimization techniques are also included in the repository – see Appendix A for details.



(a) Trajectories resulting from 0 to 4 iterations of direct single shooting. (b) Trajectories resulting from 0 to 5 iterations of direct multiple shooting.

Figure 1: Comparison of direct single shooting (a) and direct multiple shooting (b), applied to a toy dynamics problem. While direct single shooting converges in fewer iterations, each iteration takes longer than those performed in direct multiple shooting. Additionally, the parallelism of direct multiple shooting might enable it to tackle problems with longer time horizons.

4 Constrained Optimization at Scale

Nonlinear programs, such as those we constructed in Section 3, are traditionally solved using second-order techniques based on Newton’s method (Boggs and Tolle, 1995; Nocedal and Wright, 2006). To improve the computational efficiency of these methods, many software implementations such as `ipopt` and `SLSQP` leverage sparse matrix operations (Wächter and Biegler, 2006; Virtanen et al., 2020).

While effective for small models, such higher-order techniques struggle when applied over a large number of parameters, due to the size of the resulting Hessian matrix (Martens and Grosse, 2015). Many of the available libraries are also restricted to running on CPU, missing out on the massive advantages that GPU and TPU architectures have brought to deep learning (Krizhevsky et al., 2012; Abadi et al., 2016). Indeed, since GPU computation is more suitable for dense matrix operations (Fatahalian et al., 2004), the emphasis on sparsity in traditional solvers is of little help when it comes to deep learning applications. Other problems further exacerbate the challenge of using these solvers for ML: not only do higher-order techniques tend to perform poorly in high-dimensional settings due to the prevalence of saddle-points (Dauphin et al., 2014); to make matters worse, these solvers are not differentiable, making them practically impossible to use in a situations where we need to propagate gradients through the solve itself, such as meta-learning (we will explore one such setting in Section 6).

We would like to use a first-order method which can be easily integrated into an ML practitioner’s workflow, and which can take advantage of deep learning libraries and GPUs. To our knowledge, the study of constrained optimization in a deep learning context remains somewhat unexplored territory (Kotary et al., 2021). Here we present a simple technique with which we have found success on several Myriad environments.

Let f be the objective function, and h the equality constraints (depending on the trajectory optimization technique used, these could be the objective and equality constraints from Eq. (4) or Eq. (5)). We use $\mathbf{y} = [\mathbf{x}, \mathbf{u}]^\top$ to denote decision variables of the NLP (again, such as those in Eq. (4) or Eq. (5)) The Lagrangian of our NLP is then

$$\mathcal{L}(\mathbf{y}, \boldsymbol{\lambda}) = f(\mathbf{y}) + \boldsymbol{\lambda}^\top h(\mathbf{y}), \quad (6)$$

where $\boldsymbol{\lambda}$ are known as the Lagrange multipliers of the problem. We see that a solution to the NLP will correspond to the solution of the min-max game: $\min_{\mathbf{y}} \max_{\boldsymbol{\lambda}} \mathcal{L}(\mathbf{y}, \boldsymbol{\lambda})$ (Kushner and Sanvicente, 1975). In particular, this solution will satisfy the first-order optimality condition that $(D_1 \mathcal{L})(\mathbf{y}^*, \boldsymbol{\lambda}^*) = 0$ (Bertsekas, 1999). We can attempt to find a solution by applying a first-order Lagrangian method (Duguid, 1960; Uzawa et al., 1958) to find $(\mathbf{y}^*, \boldsymbol{\lambda}^*)$:

$$\begin{aligned} \mathbf{y}^{(i+1)} &\leftarrow \mathbf{y}^{(i)} - \eta_{\mathbf{y}} \cdot (D_1 f)(\mathbf{y}^{(i)}, \boldsymbol{\lambda}^{(i)}) \\ \boldsymbol{\lambda}^{(i+1)} &\leftarrow \boldsymbol{\lambda}^{(i)} + \eta_{\boldsymbol{\lambda}} \cdot (D_2 f)(\mathbf{y}^{(i)}, \boldsymbol{\lambda}^{(i)}). \end{aligned} \quad (7)$$

As an instance of gradient descent-ascent (Lin et al., 2020), this method can suffer from oscillatory and even divergent dynamics (Polyak, 1970). One way to mitigate this is the extragradient method (Korpelevich, 1976; Gidel et al., 2018). Instead of following the gradient at the current iterate, extragradient performs a “lookahead step”, effectively evaluating the gradient that would occur at a future step. It then applies the lookahead gradient to the current iterate.

$$\begin{aligned} \bar{\mathbf{y}}^{(i)} &\leftarrow \mathbf{y}^{(i)} - \eta_{\mathbf{y}} \cdot (D_1 f)(\mathbf{y}^{(i)}, \boldsymbol{\lambda}^{(i)}) \\ \bar{\boldsymbol{\lambda}}^{(i)} &\leftarrow \boldsymbol{\lambda}^{(i)} + \eta_{\boldsymbol{\lambda}} \cdot (D_2 f)(\mathbf{y}^{(i)}, \boldsymbol{\lambda}^{(i)}) \\ \mathbf{y}^{(i+1)} &\leftarrow \mathbf{y}^{(i)} - \eta_{\mathbf{y}} \cdot (D_1 f)(\bar{\mathbf{y}}^{(i)}, \bar{\boldsymbol{\lambda}}^{(i)}) \\ \boldsymbol{\lambda}^{(i+1)} &\leftarrow \boldsymbol{\lambda}^{(i)} + \eta_{\boldsymbol{\lambda}} \cdot (D_2 f)(\bar{\mathbf{y}}^{(i)}, \bar{\boldsymbol{\lambda}}^{(i)}). \end{aligned} \quad (8)$$

This approach has seen recent success in the generative adversarial model literature, and it seems likely that further improvements can be made by leveraging synergies with game-theoretic optimization (Schuermans and Zinkevich, 2016; Kodali et al., 2017; Wiatrak and Albrecht, 2019).

Trajectory Optimization – Predator Prey

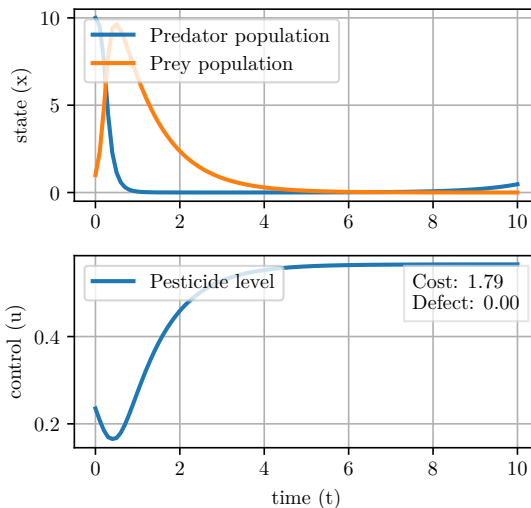


Figure 2: Optimal trajectory of pesticide use (and resulting population dynamics) in the Predator Prey domain, computed using direct single shooting.

Incorporating Inequality Constraints

For real-world systems such as those in Myriad, we want to restrict the state trajectories the agent can take. These restrictions can be expressed as bounds on the state variables of the transcribed problem. A standard way to enforce inequality constraints, which is implemented in Myriad, is via *projection*. Over the course of optimization, after a gradient step is taken, the resulting iterate is projected back into the feasible set. With fixed bounds, this can be implemented as a clip operation (Bertsekas, 1999).

An alternative, which can be included directly in the system definition, is that of *reparametrization*. Instead of stepping and then modifying the iterate to satisfy the bounds, we instead modify the space in which we are performing the optimization, so that any point in the space will be feasible (Niculae, 2020). For example, if our feasible set is $x_{\text{lower}} \leq x \leq x_{\text{upper}}$, a viable reparametrization would be to use a sigmoid of the form $\sigma(x, x_{\text{lower}}, x_{\text{upper}}) = (x_{\text{upper}} - x_{\text{lower}})/(1 + e^{-\alpha x}) - x_{\text{lower}}$, where α is a temperature constant which can be decreased over time.

5 System Identification

Sections 3 and 4 showed how to solve the trajectory optimization problem when we know the system dynamics. We now focus on the task of *learning* system dynamics from data, known as *system identification* (SysID) (Keesman, 2011).

Within the field of control theory, SysID is typically performed to learn the parameters of a highly structured model (Keesman, 2011) developed by field experts. Note that this has also been the case in recent papers at the intersection of learning and control (Amos et al., 2018; Jin et al., 2020). Not only is this task comparatively simple due to having to learn only a handful of parameters; it is also easy to verify the accuracy of the learned model by simply checking the values of the learned parameters³.

Yet the construction of a structured model relies on the ability of a human expert to accurately describe the dynamics – a difficult and lengthy process. The alternative explored in this paper is to fully infer the dynamics of a system in the form of a Neural ODE (Chen et al., 2018): a natural fit when it comes to continuous systems. While Neural ODEs have not yet been extensively studied in the context of controllable environments (Kidger et al., 2020; Alvarez et al., 2020), it is not challenging to extend them to this setting. In this case we would like to find Neural ODE parameters θ which best approximate the true dynamics:

$$f(\mathbf{x}(t), \mathbf{u}(t), \theta) \equiv \text{apply_net}(\theta, [\mathbf{x}(t), \mathbf{u}(t)]^\top) \approx f(\mathbf{x}(t), \mathbf{u}(t)), \quad (9)$$

where $f(\mathbf{x}(t), \mathbf{u}(t))$ is the true dynamics function. In order to train this model, consider a trajectory of states⁴ \mathbf{x} , sampled with noise from the true dynamics, given controls $\mathbf{u}_{0:N}$. We would like our model to predict this trajectory. In particular, $\tilde{\mathbf{x}}$ should approximate \mathbf{x} :

$$\tilde{\mathbf{x}} = \left[\mathbf{x}_0, \mathbf{x}_0 + \int_{t_0}^{t_1} f(\mathbf{x}(t), \psi(\mathbf{u}_{0:N}, t), \theta) dt, \dots, \mathbf{x}_0 + \int_{t_0}^{t_N} f(\mathbf{x}(t), \psi(\mathbf{u}_{0:N}, t), \theta) dt \right]. \quad (10)$$

³For this comparison to be meaningful, the system in question must be *identifiable*, that is, only a unique combination of parameters may lead to any given behaviour.

⁴Myriad offers several methods for generating trajectory datasets, including uniformly at random, Gaussian random walk, and sampling around a candidate control trajectory.

System Identification – Mould Fungicide

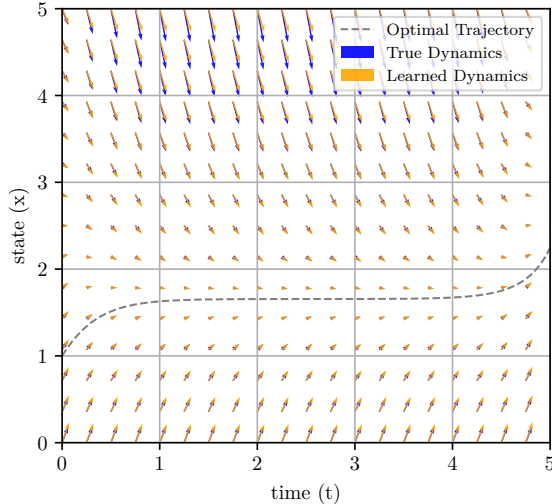


Figure 3: Comparison of true dynamics and learned dynamics (Neural ODE model) when applying optimal controls in the Mould Fungicide domain. We observe that the dynamics learned via SysID closely match the true dynamics for this problem.

We minimize the mean squared error between the two trajectories (N is number of timesteps, D is state dimension, giving \mathbf{x} and $\hat{\mathbf{x}}$ dimensions (D, N)). The loss is then calculated as⁵:

$$L(\hat{\boldsymbol{\theta}}) = \frac{1}{ND} \|\hat{\mathbf{x}} - \mathbf{x}\|_E^2, \quad (11)$$

where $\|\bullet\|_E^2$ is the squared Euclidean norm (sum of squares of elements).

In the Neural ODE setting, the individual parameters no longer convey an intuitive physical meaning. Yet, we can still compare the learned to the true dynamics by considering the effect of a given control sequence across a range of states. An example of such visualization is shown in Figure 3, which compares the Neural ODE learned model’s dynamics with those of the true dynamics on a mould fungicide domain (Lenhart and Workman, 2007). We use automatic differentiation to calculate the gradient of the loss in Eq. 11 with respect to network parameters; an alternative approach is to apply the adjoint sensitivity method as done by Chen et al. (2018).

6 End-to-End SysID and Control

As in other areas of machine learning, RL has seen increasing interest in forgoing the use of explicit models, instead structuring the policy to include a planning inductive bias such that an agent can perform *implicit* planning (Tamar et al., 2016; Deac et al., 2020; Amos et al., 2018; Jin et al., 2020). A classic example is value iteration networks (Tamar et al., 2016), which replace the explicit value iteration algorithm with an inductive bias in the form of a convolutional neural network (Fukushima, 1988; LeCun et al., 1989).

Inspired by implicit planning, we consider a fully differentiable algorithm which performs trajectory optimization on an implicit model. By propagating gradients through the trajectory optimization procedure itself, the agent can learn directly from the loss received from acting in the real environment. In order to describe this approach – a form of “unrolled optimization” (Maclaurin et al., 2015) – we consider a modification to the Lagrangian of Eq. (6), adding parameters $\boldsymbol{\theta}$ which parametrize the underlying dynamics function. We let \mathbf{y} represent the primal variables (control and state decision variables), $\boldsymbol{\lambda}$ the dual variables (Lagrange multipliers), f the objective function, and h the equality constraints⁶. To further simplify notation, we let $\mathbf{z} = [\mathbf{y}, \boldsymbol{\lambda}]^\top$, thus giving us the Lagrangian:

$$\mathcal{L}(\boldsymbol{\theta}, \mathbf{z}) = f(\mathbf{y}, \boldsymbol{\theta}) + \boldsymbol{\lambda}^\top h(\mathbf{y}, \boldsymbol{\theta}). \quad (12)$$

Let ψ be a function representing the nonlinear program solver, which takes parameter values $\hat{\boldsymbol{\theta}}$ and returns $\hat{\mathbf{z}}$, and let L be the loss function of Eq. 11. We would like to propagate the gradient of L with respect to $\hat{\boldsymbol{\theta}}$ through ψ at our current decision variables $\hat{\mathbf{y}}$. The basic procedure to achieve this is shown in Algorithm 1.

Algorithm 1 End-to-End – Theory

```

1: Initialize  $\hat{\mathbf{u}}_{0:N}$ ,  $\hat{\boldsymbol{\theta}}$  with random values
2: while  $\hat{\mathbf{u}}_{0:N}$ ,  $\hat{\boldsymbol{\theta}}$  not converged do
3:    $\hat{\mathbf{z}} \leftarrow \psi(\hat{\boldsymbol{\theta}})$  ▷ solve NLP represented by Eq. (12)
4:    $\hat{\mathbf{x}}, \hat{\mathbf{u}}_{0:N}, \hat{\boldsymbol{\lambda}} \leftarrow \hat{\mathbf{z}}$  ▷ extract controls
5:    $\hat{\boldsymbol{\theta}} \leftarrow$  update using  $(D(L \circ \psi))(\hat{\boldsymbol{\theta}})$ 
6: end while
7: return  $\hat{\mathbf{u}}_{0:N}$ 

```

The clear challenge is the implementation of Line 5. By the chain rule we have that

$$(D(L \circ \psi))(\boldsymbol{\theta}) = (DL)(\psi(\boldsymbol{\theta})) \cdot (D\psi)(\boldsymbol{\theta}). \quad (13)$$

The first term, $(DL)(\psi(\boldsymbol{\theta}))$, can simply be calculated using automatic differentiation in the imitation learning setting, or using a gradient approximation method in the RL setting (Williams, 1992). The calculation of $(D\psi)(\boldsymbol{\theta})$ is more challenging, since it involves differentiating through the NLP solver.

⁵In practice, the loss calculation is performed in parallel over a minibatch of training trajectories.

⁶For simplicity, here we present the case without inequality constraints.

A natural first approach is to apply the implicit function theorem (IFT), which suggests that for $(\boldsymbol{\theta}, \mathbf{z})$ such that $\mathbf{z} = \psi(\boldsymbol{\theta})$ and $(D_1 \mathcal{L})(\boldsymbol{\theta}, \mathbf{z})$ is near zero, we have

$$(D \psi)(\boldsymbol{\theta}) = -(D_2 D_1 \mathcal{L})^{-1}(\boldsymbol{\theta}, \mathbf{z}) \cdot (D_1^2 \mathcal{L})(\boldsymbol{\theta}, \mathbf{z}). \quad (14)$$

In practice, we experienced several drawbacks when using this method. Most notably, we found the requirement that $(D_1 \mathcal{L})(\boldsymbol{\theta}, \mathbf{z})$ be near zero in order for the implicit function theorem to hold particularly challenging, since an unreasonable amount of computation must be spent to achieve such high accuracy from the NLP solver.

A practical solution is to use a *partial* solution at each timestep, and take gradients through an unrolled differentiable NLP solver. By performing several gradient updates per iteration and warm-starting each step at the previous iterate, we are able to progress towards an optimal solution while staying computationally feasible. We reset the warm-start after a large number of iterations, as in (Jin et al., 2020), to avoid catastrophic forgetting of previously-seen dynamics. This approach is presented in Algorithm 2.

Algorithm 2 End-to-End Approach – Practice

```

1: Initialize  $\hat{\mathbf{u}}_{0:N}, \hat{\boldsymbol{\theta}}$  with random values
2: while  $\hat{\mathbf{u}}_{0:N}, \hat{\boldsymbol{\theta}}$  not converged do
3:    $\hat{\mathbf{z}}, \mathbf{dz\_dtheta} \leftarrow$  simultaneously take several steps of  $\psi(\hat{\boldsymbol{\theta}})$  and accumulate gradients
4:    $\hat{\mathbf{x}}, \hat{\mathbf{u}}_{0:N}, \hat{\boldsymbol{\lambda}} \leftarrow \hat{\mathbf{z}}$  ▷ extract controls
5:    $\mathbf{dL\_dz} \leftarrow (D L)(\hat{\mathbf{z}})$  ▷ using automatic differentiation or gradient approximation
6:    $\mathbf{dL\_dtheta} \leftarrow \mathbf{dL\_dz} \cdot \mathbf{dz\_dtheta}$  ▷ apply the chain rule
7:    $\hat{\boldsymbol{\theta}} \leftarrow$  update with  $\mathbf{dL\_dtheta}$ 
8: end while
9: return  $\hat{\mathbf{u}}_{0:N}$ 

```

We find that Algorithm 2 is able to learn effective models and propose good controls on several environments. To gain intuition about how the model learns its environment over time, we take snapshots of the controls proposed by our algorithm over the course of training. We show an example of this in Figure 4, which shows the progress of end-to-end training of a Neural ODE model on a cancer treatment domain (Lenhart and Workman, 2007).

End-to-End Model Learning – Cancer Treatment

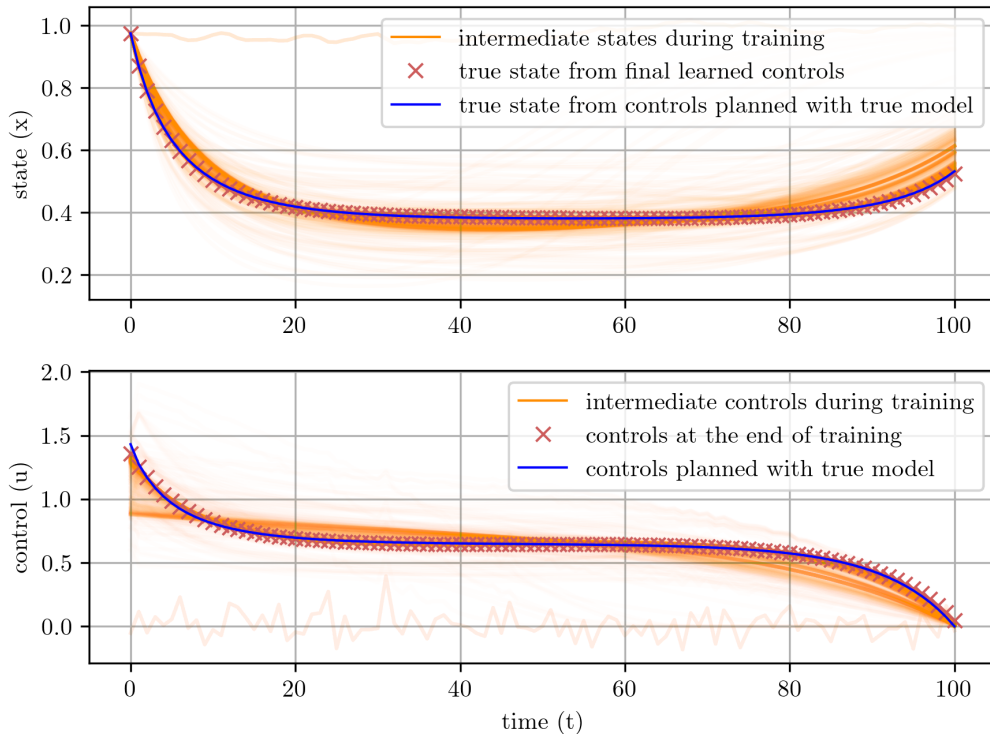


Figure 4: Visualization of how the controls, and corresponding states, evolve over the course of training a Neural ODE model end-to-end on the Cancer Treatment domain. The control trajectory, and corresponding state trajectory, are sampled regularly over the course of training. Each is plotted with a low alpha value to show where the learning procedure spent time during training.

7 Conclusion

We have presented the Myriad repository, a testbed for trajectory optimization and continuous-time dynamics learning which can easily be incorporated into a machine learning workflow. After presenting the general code layout and features of the repository, we discussed trajectory optimization and system identification, two tasks which can be easily done at scale using the tools in Myriad. Finally, we developed an end-to-end approach to train a control-oriented implicit-planning imitation learning agent, which leverages Myriad’s unique integration of trajectory optimization techniques with powerful and versatile deep learning machinery.

It is our hope that Myriad will serve as a stepping stone towards increased interest for ML to be inspired by, and developed for, impactful real-world settings.

Acknowledgements

Thank you to Lama Saouma for input regarding the feasibility of an end-to-end approach for SysID and Control. Thank you to Andrei M. Romascanu for feedback on an earlier version of this manuscript.

References

Abadi, M., Barham, P., Chen, J., Chen, Z., Davis, A., Dean, J., Devin, M., Ghemawat, S., Irving, G., Isard, M., Kudlur, M., Levenberg, J., Monga, R., Moore, S., Murray, D. G., Steiner, B., Tucker, P., Vasudevan, V., Warden, P., Wicke, M., Yu, Y., and Zheng, X. (2016). Tensorflow: A system for large-scale machine learning. In *12th USENIX Symposium on Operating Systems Design and Implementation (OSDI 16)*, pages 265–283.

- Altman, E. (1999). *Constrained Markov decision processes*, volume 7. CRC Press.
- Alvarez, V. M. M., Rosca, R., and Falcutescu, C. G. (2020). Dynode: Neural ordinary differential equations for dynamics modeling in continuous control. *arXiv preprint arXiv:2009.04278*.
- Amos, B., Rodriguez, I. D. J., Sacks, J., Boots, B., and Kolter, J. Z. (2018). Differentiable mpc for end-to-end planning and control. In *Proceedings of the 32nd International Conference on Neural Information Processing Systems, NIPS'18*, page 8299–8310, Red Hook, NY, USA. Curran Associates Inc.
- Antony, T. (2018). *Large Scale Constrained Trajectory Optimization Using Indirect Methods*. PhD thesis, Purdue University.
- Bellemare, M. G., Naddaf, Y., Veness, J., and Bowling, M. (2013). The arcade learning environment: An evaluation platform for general agents. *Journal of Artificial Intelligence Research*, 47:253–279.
- Bertsekas, D. P. (1999). *Nonlinear programming*. Athena Scientific.
- Betts, J. T. (2010). *Practical methods for optimal control and estimation using nonlinear programming*. Siam.
- Biegler, L. (2010). *Nonlinear Programming: Concepts, Algorithms, and Applications to Chemical Processes*.
- Boggs, P. T. and Tolle, J. W. (1995). Sequential quadratic programming. *Acta numerica*, 4:1–51.
- Bradbury, J., Frostig, R., Hawkins, P., Johnson, M. J., Leary, C., Maclaurin, D., Necula, G., Paszke, A., VanderPlas, J., Wanderman-Milne, S., and Zhang, Q. (2018). JAX: composable transformations of Python+NumPy programs.
- Chen, T. Q., Rubanova, Y., Bettencourt, J., and Duvenaud, D. (2018). Neural ordinary differential equations. *CoRR*, abs/1806.07366.
- Dauphin, Y. N., Pascanu, R., Gulcehre, C., Cho, K., Ganguli, S., and Bengio, Y. (2014). Identifying and attacking the saddle point problem in high-dimensional non-convex optimization. *Advances in neural information processing systems*, 27.
- Deac, A., Veličković, P., Milinković, O., Bacon, P.-L., Tang, J., and Nikolić, M. (2020). Xlvin: executed latent value iteration nets. *arXiv preprint arXiv:2010.13146*.
- Deng, J., Dong, W., Socher, R., Li, L.-J., Li, K., and Fei-Fei, L. (2009). ImageNet: A Large-Scale Hierarchical Image Database. In *CVPR09*.
- Duguid, A. (1960). Studies in linear and non-linear programming, by k. j. arrow, l. hurwicz and h. uzawa. stanford university press, 1958. 229 pages. *Canadian Mathematical Bulletin*, 3(3):196–198.
- Fatahalian, K., Sugerman, J., and Hanrahan, P. (2004). Understanding the efficiency of gpu algorithms for matrix-matrix multiplication. In *Proceedings of the ACM SIGGRAPH/EUROGRAPHICS conference on Graphics hardware*, pages 133–137.
- Fehlberg, E. (1969). *Low-order classical Runge-Kutta formulas with stepsize control and their application to some heat transfer problems*, volume 315. National aeronautics and space administration.
- Fukushima, K. (1988). Neocognitron: A hierarchical neural network capable of visual pattern recognition. *Neural networks*, 1(2):119–130.
- Gidel, G., Berard, H., Vignoud, G., Vincent, P., and Lacoste-Julien, S. (2018). A variational inequality perspective on generative adversarial networks. *arXiv preprint arXiv:1802.10551*.
- Henderson, P., Islam, R., Bachman, P., Pineau, J., Precup, D., and Meger, D. (2018). Deep reinforcement learning that matters. In *Proceedings of the AAAI conference on artificial intelligence*, volume 32.
- Jin, W., Wang, Z., Yang, Z., and Mou, S. (2020). Pontryagin differentiable programming: An end-to-end learning and control framework. In Larochelle, H., Ranzato, M., Hadsell, R., Balcan, M., and Lin, H., editors, *Advances in Neural Information Processing Systems 33: Annual Conference on Neural Information Processing Systems 2020, NeurIPS 2020, December 6-12, 2020, virtual*.
- Keesman, K. J. (2011). *System identification: an introduction*. Springer Science & Business Media.
- Kelly, M. (2017). An introduction to trajectory optimization: How to do your own direct collocation. *SIAM Review*, 59(4):849–904.

- Kerner, H. (2020). Too many ai researchers think real-world problems are not relevant. *Opinion. MIT Technology Review*.
- Kidger, P., Morrill, J., Foster, J., and Lyons, T. (2020). Neural controlled differential equations for irregular time series. *arXiv preprint arXiv:2005.08926*.
- Kodali, N., Abernethy, J., Hays, J., and Kira, Z. (2017). On convergence and stability of gans. *arXiv preprint arXiv:1705.07215*.
- Koh, P. W., Sagawa, S., Marklund, H., Xie, S. M., Zhang, M., Balsubramani, A., Hu, W., Yasunaga, M., Phillips, R. L., Gao, I., Lee, T., David, E., Stavness, I., Guo, W., Earnshaw, B. A., Haque, I. S., Beery, S., Leskovec, J., Kundaje, A., Pierson, E., Levine, S., Finn, C., and Liang, P. (2021). WILDS: A benchmark of in-the-wild distribution shifts. In *International Conference on Machine Learning (ICML)*.
- Korpelevich, G. (1976). An extragradient method for finding saddle points and for other problems.
- Kotary, J., Fiochetto, F., Van Hentenryck, P., and Wilder, B. (2021). End-to-end constrained optimization learning: A survey. *arXiv preprint arXiv:2103.16378*.
- Krizhevsky, A., Sutskever, I., and Hinton, G. E. (2012). Imagenet classification with deep convolutional neural networks. *Advances in neural information processing systems*, 25:1097–1105.
- Kushner, H. J. and Sanvicente, E. (1975). Stochastic approximation of constrained systems with system and constraint noise. *Automatica*, 11(4):375–380.
- LeCun, Y., Boser, B., Denker, J. S., Henderson, D., Howard, R. E., Hubbard, W., and Jackel, L. D. (1989). Backpropagation applied to handwritten zip code recognition. *Neural computation*, 1(4):541–551.
- Leike, J., Krueger, D., Everitt, T., Martic, M., Maini, V., and Legg, S. (2018). Scalable agent alignment via reward modeling: a research direction. *CoRR*, abs/1811.07871.
- Lenhart, S. and Workman, J. T. (2007). *Optimal control applied to biological models*. Chapman & Hall/CRC.
- Lin, T., Jin, C., and Jordan, M. (2020). On gradient descent ascent for nonconvex-concave minimax problems. In *International Conference on Machine Learning*, pages 6083–6093. PMLR.
- Maclaurin, D., Duvenaud, D., and Adams, R. (2015). Gradient-based hyperparameter optimization through reversible learning. In *International conference on machine learning*, pages 2113–2122. PMLR.
- Martens, J. and Grosse, R. B. (2015). Optimizing neural networks with kronecker-factored approximate curvature. In Bach, F. R. and Blei, D. M., editors, *Proceedings of the 32nd International Conference on Machine Learning, ICML 2015, Lille, France, 6-11 July 2015*, volume 37 of *JMLR Workshop and Conference Proceedings*, pages 2408–2417. JMLR.org.
- Nicolae, V. (2020). Optimizing with constraints: reparametrization and geometry.
- Nocedal, J. and Wright, S. (2006). *Numerical Optimization: Springer Series in Operations Research and Financial Engineering*. Springer.
- Polyak, B. (1970). Iterative methods using lagrange multipliers for solving extremal problems with constraints of the equation type. *USSR Computational Mathematics and Mathematical Physics*, 10(5):42–52.
- Schuermans, D. and Zinkevich, M. A. (2016). Deep learning games. In *Advances in Neural Information Processing Systems*, pages 1678–1686.
- Tamar, A., Wu, Y., Thomas, G., Levine, S., and Abbeel, P. (2016). Value iteration networks. *arXiv preprint arXiv:1602.02867*.
- Tedrake, R., Development Team1, D., and Development Team2, D. (2019). Drake: Model-based design and verification for robotics.
- Todorov, E., Erez, T., and Tassa, Y. (2012). Mujoco: A physics engine for model-based control. In *2012 IEEE/RSJ International Conference on Intelligent Robots and Systems*, pages 5026–5033. IEEE.
- Uzawa, H., Anow, K., and Hurwicz, L. (1958). Studies in linear and nonlinear programming.

- Virtanen, P., Gommers, R., Oliphant, T. E., Haberland, M., Reddy, T., Cournapeau, D., Burovski, E., Peterson, P., Weckesser, W., Bright, J., van der Walt, S. J., Brett, M., Wilson, J., Millman, K. J., Mayorov, N., Nelson, A. R. J., Jones, E., Kern, R., Larson, E., Carey, C. J., Polat, İ., Feng, Y., Moore, E. W., VanderPlas, J., Laxalde, D., Perktold, J., Cimrman, R., Henriksen, I., Quintero, E. A., Harris, C. R., Archibald, A. M., Ribeiro, A. H., Pedregosa, F., van Mulbregt, P., and SciPy 1.0 Contributors (2020). SciPy 1.0: Fundamental Algorithms for Scientific Computing in Python. *Nature Methods*, 17:261–272.
- Wächter, A. and Biegler, L. T. (2006). On the implementation of an interior-point filter line-search algorithm for large-scale nonlinear programming. *Mathematical programming*, 106(1):25–57.
- Wiatrak, M. and Albrecht, S. V. (2019). Stabilizing generative adversarial network training: A survey.
- Williams, R. J. (1992). Simple statistical gradient-following algorithms for connectionist reinforcement learning. *Machine learning*, 8(3):229–256.

A Myriad Environments, Optimizers, Integration Methods

Name	Brief Description	Fixed x_T	Terminal Cost
Bacteria*	Manage bacteria population levels	No	Yes
Bear Populations*	Manage metapopulation of bears	No	No
Bioreactor*	Grow bacteria population	No	No
Cancer Treatment*	Decrease tumour size via chemotherapy	No	No
Cart-Pole Swing-Up	Swing up pendulum by translating pivot	Yes	No
Epidemic*	Control epidemic via vaccination	No	No
Glucose*	Manage blood glucose via insulin injections	No	No
Harvest*	Maximize harvest yield	No	No
HIV Treatment*	Manage HIV via chemotherapy	No	No
Mould Fungicide*	Control mould population via fungicide	No	No
Mountain Car	Drive up valley with limited force	Yes	No
Pendulum	Swing up pendulum by rotating pivot	Yes	No
Predator Prey*	Minimize pest population	Yes	Yes
Rocket Landing	Land a rocket	Yes	No
Timber Harvest*	Optimize tree harvesting	No	No
Tumour*	Block tumour blood supply	No	Yes
Van Der Pol	Forced Van der Pol oscillator	Yes	No

Table 1: The environments currently available in the Myriad repository. Environments with an (*) were inspired by corresponding examples described by Lenhart and Workman (2007). Some environments require that the system end up in a specific state at the end of an episode. Additionally, some environments impose a cost additional to the instantaneous cost, evaluated based on the system’s final state.

Method Name	Direct / Indirect	Sequential / Parallel	Integration Method
Single Shooting	Direct	Sequential	Any
Multiple Shooting	Direct	Partially Parallel	Any
Trapezoidal Collocation	Direct	Parallel	Trapezoidal Rule
Hermite-Simpson Collocation	Direct	Parallel	Simpson’s Rule
Forward-Backward Sweep	Indirect	Sequential	Runge-Kutta 4th Order

Table 2: The trajectory optimization techniques available in the Myriad repository. Direct techniques discretize the control problem and solve the resulting nonlinear program. Indirect methods first augment the problem with an adjoint equation, before discretizing and solving.

Integration Method	Explicit / Implicit	Gradient Evaluations
Euler	Explicit	1
Heun	Explicit	2
Midpoint	Explicit	2
Runge-Kutta 4th Order	Explicit	4
Trapezoidal	Implicit	NA
Simpson	Implicit	NA

Table 3: The integration methods available in the Myriad repository.